

Comparison of Electrical Power for Thermoelectric Oxide Module

Melania Suweni Muntini^a, Risse Entikaria Rachmanita^a, Diky Anggoro^a,
Irasani Rahayu^a, Nanda rico Famas Putra^a, Nilna Fauziah^a, Sylvia Junior Susanto^a,
Meylusari Maghfirotul Afiyanti^a, Panida Pilasuta^{b,c}, Supasit Paengson^{b,c},
Wanachaporn Namhongsa^{b,c}, Surasak Ruamruk^{b,c}, Soe ko ko Aung^d, Kunchit Singsoog^{b,c,*}

^aInstrumentation and electronic laboratory, Department of physics, Institut teknologi sepuluh nopember, Surabaya, 60111 East java Indonesia

^bThermoelectric Research Laboratory, Center of excellence on Alternative Energy, Research and Development Institute, Sakon Nakhon Rajabhat University, 680 Nittayo Road, Mueang District, Sakon Nakhon, 47000 Thailand

^cProgram of Physics, Faculty of Science and Technology, Sakon Nakhon Rajabhat University, 680 Nittayo Road, Mueang District, Sakon Nakhon, 47000 Thailand

^dDepartment of Physics, University of Yangon, Pyay Road, Kamaryut Township, Yangon 11041 Myanmar

Received 15 November 2017; Revised 25 November 2017; Accepted 30 November 2017

Abstract

The thermoelectric (TE) module was fabricated by 4 pairs of p-Ca₃Co₄O₉ + Ag 10 wt% (CCO) and n-Ca_{0.97}Bi_{0.03}MnO₃ (CMO) legs. The CCO and CMO legs were synthesized by hot-press (HP) method and measuring TE properties in temperature ranges 300 – 473 K in air. The heat transfer and electric behavior in boundary temperature were analyzed by the finite element method (FEM). The simulation results are electrical power according to all values of experiment data. The efficiency of TE module depended on heat loss, current loss, distance between TE legs and shape of electrode. The maximum electric power of simulation is 56 mW at different temperature 200 K.

KEYWORDS: Thermoelectric materials; Thermoelectric properties; Numerical simulation; Calcium Cobalt Oxide; Calcium Manganese Oxide

* Corresponding authors; e-mail: kunchitsingsoog@yahoo.com

Introduction

Thermoelectric (TE) module has been converted heat into electricity and reversed electricity to different temperature between top and bottom side of TE module. The performance of TE material depend on dimensionless figure of merit value ($ZT = S^2\rho T/\kappa$, where S is Seebeck coefficient, ρ is electrical resistivity, T is absolute temperature and κ is thermal conductivity). In case of thermoelectric generator, there are many condition affect to output power such as shape of TE leg [1, 2], number of p-n pair [3], the properties of materials, temperature and load resistance [4] etc. Therefore, these conditions are major main for thermoelectric fabrication. Finite element method (FEM) is a numerical method for solving problems of engineering and mathematical physics. It's also used for simulating heat transfer and electric behavior of TE module [5 – 10]. The thermoelectric system of finite element equations can be written by Eq. (1).

$$\begin{bmatrix} C^{TT} & 0 \\ 0 & C^{\varphi\varphi} \end{bmatrix} \begin{bmatrix} \bar{T}_e \\ \bar{\varphi}_e \end{bmatrix} + \begin{bmatrix} K^{TT} & 0 \\ K^{\varphi T} & K^{\varphi\varphi} \end{bmatrix} \begin{bmatrix} \bar{T}_e \\ \bar{\varphi}_e \end{bmatrix} = \begin{bmatrix} \bar{Q} + \bar{Q}^p + \bar{Q}^e \\ I \end{bmatrix} \quad (1)$$

where C^{TT} is thermal damping matrix, $C^{\varphi\varphi}$ is dielectric damping matrix, K^{TT} is thermal stiffness matrix, $K^{\varphi T}$ is Seebeck stiffness matrix, $K^{\varphi\varphi}$ is electric stiffness matrix, \bar{Q} is vector of combined heat generation loads, \bar{Q}^p is Peltier heat load vector and \bar{Q}^e is electric power load vector.

In this work, the objectives are to predict temperature distribution, electric voltage and heat flux for understanding thermal and electrical behavior of thermoelectric module and developing thermoelectric efficiency.

Materials and Methods

TE Module fabrication

The n-Ca_{0.97}Bi_{0.03}MnO₃ and p-Ca₃Co₄O₉ + Ag 10 wt% were synthesized by ball mill and hot press method. The starting materials were mixed by planetary ball mill for 2 h at 350 rpm in atmosphere. The mixed powders of n and p materials were loaded into graphite die in diameter 20 mm after that they press 1 MPa and heat at 1073 K (n) and 923 K (p) for 1 h in Ar gas into pellets. The pellet was cut in size of 4×4×4 mm³ and fabricated TE module using Cu electrode, alumina substrate for 4 p-n couples connected by melting solder method. The electrical power of TE module was measured as shown in Fig. 1.

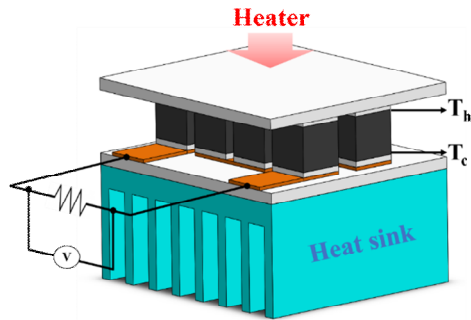


Fig. 1 The schematic diagram measured electrical power of TE module.

TE module simulation

The TE module was designed by FEM simulation using the n-p legs in size of 4×4×4 mm³, Cu electrode thickness 0.3 mm, alumina substrate size 20×22×1 mm³, solder thickness 0.5 mm and automatic generating mesh are shown in Fig. 2. The Seebeck coefficient, electrical resistivity and thermal conductivity of p and n materials to design TE model are shown in Table 1. The temperature conditions were applied to top (36 – 226 °C) and bottom (26 °C) of TE module. The electrical current and output electrical power were simulated by using resistor connected between first p leg and last n leg of TE module. In addition, the zero set of voltage was assigned on electrode of final n leg for generated temperature distribution, electric voltage, heat flux and current density.

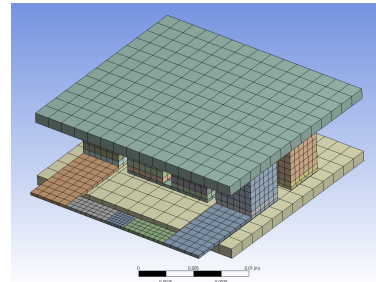


Fig. 2 Generating mesh of TE module design

Table 1 The thermoelectric properties of law materials of TE module design.

Materials	Temperature (°C)	Seebeck coefficient (μV/K)	Electrical resistivity (mΩ cm)	Thermal conductivity (W/m K)
CCO	50	131.69	3.47	4.40
	100	154.68	3.19	3.69
	150	189.29	2.89	3.25
	200	239.77	2.65	2.84
CMO	50	-121.97	6.82	4.70
	100	-162.65	7.70	4.45
	150	-187.46	8.40	4.10
	200	-226	9.06	3.60
Cu	constant	-	1.23×10 ⁻²	400
Alumina	constant	-	-	35
Solder	constant	-	1.23×10 ⁻²	55

Results and Discussion

Temperature distribution

Figure 3 shows the smooth temperature distribution decreasing from top to bottom by thermal conductivity of n and p legs. The phenomenon was described two contact solid materials by heat flows from the hotter body to the colder body because the thermal contact resistance existing between the contacting surfaces [11]. The heat flow between two bodies are described by Fourier's law following by Eq. (2)

$$q = -\kappa A \frac{dT}{dx} \quad (2)$$

where q is the heat flow, κ is the thermal conductivity, A is the cross-sectional area and dT/dx is the temperature gradient in the direction of flow. We considered the energy conservation to find the heat flow between the two bodies A and B by Eq. (3);

$$q = \frac{T_1 - T_2}{\Delta x_A / (\kappa_A A) + 1 / (h_c A) + \Delta x_B / (\kappa_B A)} \quad (3)$$

It can be seen that the heat flow was directly related to the thermal conductivities of the bodies in contact (κ_A and κ_B), the contact area (A), the thermal contact resistance ($1/h_c$) and inverse the thermal conductance coefficient (h_c)

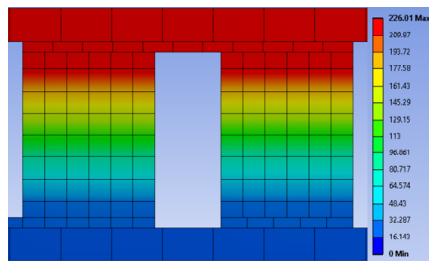


Fig.3 Temperature distribution of TE module at different temperature 200 K

Electric voltage

The simulation of electrical voltage as a function of different temperature is shown in Fig. 4 corresponding with experimental data. The maximum electrical voltage is 0.23 V at different temperature 200 K using relationship of Seebeck coefficient and different temperature following by Eq. (4).

$$V = S\Delta T \quad (4)$$

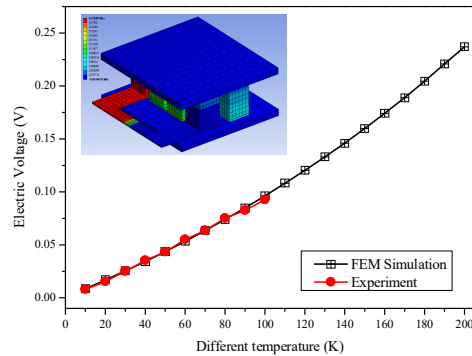


Fig. 4 Electrical voltage of TE module at different temperature 200 K.

Total heat flux

Figure 5 shows total heat flux in proportional vector display observed at the corner of TE materials and more area heat absorption from substrate. Moreover, heat loss can be observed in space between TE legs because ambient temperature was set in simulation and heat was exchanged with milieu. The TE module efficiency depended on substrate size and distance of TE legs.

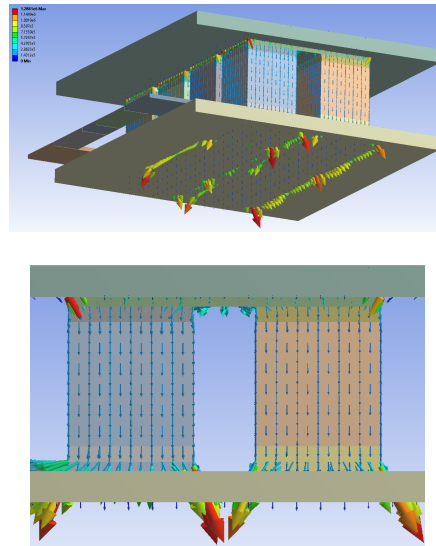


Fig. 5 Total heat flux of thermoelectric module at $T_h = 226 \text{ }^\circ\text{C}$ and $T_c = 26 \text{ }^\circ\text{C}$.

Total current density

Figure 6 shows that total current density in uniform vector display which observed on conducting materials including to Cu electrode, solder, p and n materials. The current vectors losses were distinguished especially in Cu between TE

legs and the shape of electrode should be various for studying behavior of current vector.

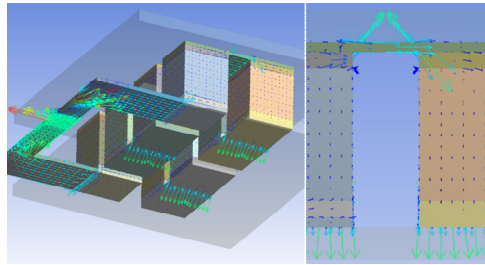


Fig. 6 Total current density of thermoelectric module at $T_h = 226\text{ }^\circ\text{C}$ and $T_c = 26\text{ }^\circ\text{C}$.

Electric power

The relationship between different temperature and output power in the simulation corresponding with experimental data are shown in Fig. 7. The maximum output power for experiment and simulation results are 8.57 and 9.28 mW respectively at different temperature 100 K. However, the output power in the simulation is higher than experimental value due to Ohmic contacts on p - n junction materials were affected. The maximum power of TE module for simulation is 56.2 mW at different temperature 200 K.

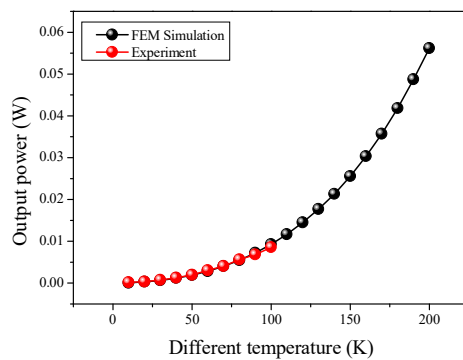


Fig. 7 Output power as a function of different temperature of TE module

Conclusion

The TE materials and TE module were successfully prepared by HP and melting solder method respectively. The results in the FEM simulation including temperature distribution, electrical voltage, heat flux, current density, output power, heat loss and current vector loss were significantly predicted. The distance between TE legs and shape of electrode were affected to efficiency of TE module. However,

both the electrical voltage and output power were corresponded with experimental data and increased with increasing different temperature. The maximum electrical voltage and output power of TE module in the simulation are 0.23 V and 56.2 mW respectively at different temperature 200 K. The FEM simulation was predicted by the thermal and electrical behavior of TE module.

References

- [1] A. Fabián-Mijangos, G. Min, J. Alvarez-Quintana, Enhanced performance thermoelectric module having asymmetrical legs, *Ener. Conver. Manag.* 148 (2017) 1372 – 1381.
- [2] B. Jang, S. Han, J-Y. Kim, Optimal design for micro-thermoelectric generators using finite element analysis, *Micro. Engn.* 88 (2011) 775 – 778.
- [3] K. Singsoog, C. Thanachayanont, A. Charoenphakdee, T. Seetawan, Thermoelectric Properties and Power Generation of p-Ca₃Co₄O₉ and n-Sr_{0.87}La_{0.13}TiO₃ Thermoelectric Modules, *Key Eng. Mater.* 675–676 (2016) 679 – 682.
- [4] P. Ziolkowski, P. Poinas, J. Leszczynski, G. Karpinski, E. Muller, Estimation of Thermoelectric Generator Performance by Finite Element Modeling, *J. Electro. Mater.* 39 (2010) 1934 – 1943.
- [5] G. Wu, X. Yu, A Comprehensive 3D Finite Element Model of a Thermoelectric Module Used in a Power Generator: A Transient Performance Perspective, *J. Electro Mater.* 44 (2015) 2080 – 2088.
- [6] G. Wua, X. Yu, A holistic 3D finite element simulation model for thermoelectric power generator element, *Ener. Conver. Manag.* 86 (2014) 99 – 110.
- [7] S. Palaniappana, B. Palanisamy, Finite element analysis of thermoelectric refrigeration system, *Procedia Engineer.* 64 (2013) 1056 – 1061.
- [8] S. Turenne, T. Clin, D. Vasilevskiy, R.A. Masut, Finite Element Thermomechanical Modeling of Large Area Thermoelectric Generators based on Bismuth Telluride Alloys, *J. Electro Mater.* 39 (2010) 1926 – 1933.
- [9] E. Sandoz-Rosado, R. Stevens, Robust Finite Element Model for the Design of Thermoelectric Modules, *J. Electro Mater.* 39 (2010) 1848 – 1855.

- [10] L-L. Liao, M-J. Dai, C-K. Liu, K-N. Chiang, Thermo-electric finite element analysis and characteristic of thermoelectric generator with intermetallic compound, *Micro. Engn.* 120 (2014) 194 – 199.
- [11] J.P. Holman, *Heat Transfer*. 8th Edition, McGraw-Hill, Inc., New York, 1997.